Laser Dimpling and Remote Welding of Zinc Coated Steels for Automotive Applications

Daniele Colombo*, Barbara Previtali

Politecnico di Milano, Mechanical Engineering Department

Via La Masa 1, Milano (MI), Italy

*corresponding author: daniele.colombo@polimi.it

Abstract

The flexibility in terms of beam shapebility and amplitude in the range of process parameters offered by the emerging high power and quality active fiber lasers can be advantageously used in overcoming the well-known problems in remote laser welding of zinc coated steel components in the car mass production. The paper explores the potentiality offered by the combination of the scanner technology with high brilliance fiber lasers when laser dimpling and remote welding are executed in a successive order, the first one to realize gap spacers, the second one to weld together clamped sheets in zinc coated steels. In particular, the substitution of the traditional mechanical dimpling with the laser dimpling is investigated in order to highlight the potentiality of a solution that is flexible, unaffected by tool wear and highly productive.

Keywords: Remote Laser Welding, Laser Dimpling, Zinc-coated steels, Zinc-venting

1. INTRODUCTION

Laser welding is gradually replacing traditional forms of welding across many applications in automotive production and even if laser brazing [1] and remote laser cutting [2] are receiving more attention, remote laser welding (RLW) can be considered the most established laser welding process.

RLW is a contactless welding procedure. A long focal length is used to focus the laser beam at relatively high distances in a very fast beam movement in order to perform weld beads at high welding speed without the supply of shielding gas or welding filler material. Typical focal lengths are between 200 mm and 500 mm; however remote laser processes with longer focal length have been demonstrated [3]. Thanks to the rapid diffusion of high power active fiber laser sources, RLW capabilities are highly enhanced. Active fiber lasers can be focused to a small spot also with long focal lengths and, along with the high achievable laser powers, keyhole welding mode can be easily obtained [4-6].

Different materials can be laser welded in different remote welding configurations. Among them, a common welding process in the automotive production is the laser welding of zinc-coated steel in lap-joint configuration [5-7]; however the complexity of laser welding of zinc-coated steels could induce a number of welding defects that prevent a wider implementation of the technology at an industrial level.

It is well known indeed that to achieve a high-quality weld on galvanized steels in lap joint configuration is difficult by RLW because of the presence of highly pressurized zinc vapour. In fact, the boiling point of zinc is 906°C, much lower than the melting point of steels (over 1500°C), therefore during laser welding of galvanized steels in a gap-free lap joint configuration, highly pressurized zinc vapor is easily developed at the interface of the two metal sheets. This highly pressurized zinc vapor expels the liquid metal out of the molten pool and produces weld defects such as spatter and porosity during the laser welding process, finally degrading the mechanical properties of the weld joints [6].

Different solutions were adopted in order to prevent defects occurring due to zinc vapor during RLW of zinc-coated steels. Among them, investigated solutions were based on: i) the introduction of aluminum foil between the zinc-coated surface to increase the temperature at which Al-Zn composites vaporize [8-9], ii) the use of active welding gases to increase the weld bead temperature to enlarge the keyhole [6], iii) the adoption of hybrid welding systems to warrant preheating of the

zinc coating and its evaporation prior to the welding process [10], iv) the adoption of bifocal focusing lenses [11], laser knurling [12], dual beam laser welding procedures to enlarge the keyhole in the welding direction and allow degassing of zinc vapors [12-15], v) the control of the molten shape based on pulsed wave laser welding regime with both Nd:YAG laser [16] and CO_2 laser [17], and power modulation to control keyhole oscillation [18-20].

Even if the feasibility of all these solution was experimentally demonstrated, their adoption in industrial production is far to be accepted, mainly because of their complexity and costs. The only solution that is nowaday industrially adopted to prevent defects from zinc vapors is based on the use of a gap between the overlapped sheets to allow degassing of zinc vapors, where the value of the gap is generally selected according to the thicknesses of both the metal sheets and the zinc coating [21]. A standard solution for gap control is obtained by stamping on the lower plates circular bosses whose height define the gap. However it has been shown that the risk of generating holes and pores is high when the boss height is too small (<50 μm); on the contrary, the risk of unacceptable top bead depression increases if the boss height is too high (>200 μm) [3].

On the contrary, a novel and most promising solution is based on the laser dimpling procedure. The same laser equipment that provides RLW can generate a positive protrusion of molten material, hereafter dimple. The dimples act as zinc degassing points during RLW process imposing a constant gap to the clamped sheets.

However little data is available on the scientific literature about this technique, that is able to produce dimples with height varying between 50 μm and 300 μm, depending on the used laser parameters [22]. The possibility to realize gap venting features making use of the same laser source and scanner head devoted to the RLW process is very intriguing because it adds flexibility and potentiality to the entire assembling phase. Contrary to the tools and dies used in the stamping, the laser beam does not suffer of progressive wear. Moreover shape, height, position and numbers of the dimples are not rigidly pre-determined but can be varied by varying the laser process parameters and commanding opportunely the scanner head. The use of a scanner head for laser dimpling indeed has evident advantages given by the flexibility in terms of process parameters and by the high productivity achievable thanks to high scanning speeds and, as already said, by the absence of wear and deformation of the laser tool.

2. AIM OF THE PAPER AND REPRESENTATIVE CASE STUDY

In the paper an integrated solution that includes laser dimpling and then remote laser welding, is investigated. Principal aim is to investigate the feasibility of the dimples as gap-venting features when RLW is performed on zinc coated sheets clamped together and spaced by the dimples themselves.

As schematically illustrated in Fig. 1, in the paper two distinct phases are investigated:

a) Pre-processing phase, i.e. dimpling, where adequate dimples are accomplished by the same laser source and equipment that are planned to remote laser welding the zinc coated steels once dimpled;
b) Processing-phase, i.e. welding phase, where the adequate quality attributes of the welded joints are sought in order to guarantee the respect of the automotive standards imposed by the car manufacturer.

Insert Figure 1 here

The industrial context of remote fiber laser welding is reproduced that means the industrial specifications and constraints typical of the automotive sector are considered during the experimentation.

In the case of the dimpling phase the most critical attribute is the dimple height that ensures a constant distance between the two sheets. The same specification, used for the mechanical boss stamping, is adopted in terms of dimple height. Since the physical phenomenon regulating the dimple formation and consequently the dimple height is quite complex and unknown, an experimental approach is preferred and a regression model relating the dimple height to the main laser process parameters is investigated.

In the case of the RLW, the specifications and quality attribute of the lap joints are better known. These attributes principally regulate the joint dimensions and soundness. As in the case of laser dimpling an experimental approach is used to determine the main relationship between the laser process parameters and the joint dimensions.

A scheme of the dimpling and welding configuration is presented in Fig. 2, while the most common key process indicators used for the evaluation of the weld bead quality in remote laser welding of overlapped zinc coated steel are generally the

ones directly related to the mechanical properties of the joint [23-24]. As for the specifications of these key process indicators, their selection and real relationship with joint strength is still under exploration. In fact, unlike the more traditional resistance spot welding process where a great deal of work has been conducted, information on a remote laser beam weld is nowadays sparse. In industrial practice automotive manufacturers use their own specifications for the chosen key process indicators. Accordingly, in the presented work, proprietary specifications of industrial partners have been selected as follows:

1. Dimple height, H. For such a welding configuration zinc venting requires a certain gap between the overlapped sheets. The required dimple height (H) has to be properly tuned to match the gap value (G). Standard gap values ranges between 50-200 μm depending on the upper and lower sheet thickness [22] and a nominal value of the gap of 100 μm is generally required when the upper sheet has a thickness lower than 1 mm. In the mechanical stamping variability in the boss height of about 20% gap thickness is allowed in order to take into consideration stamping process variability and die wear. Similar tolerance is assumed in the case of laser dimpling.

2. Dimensions of the remote laser welded joint in the cross section. The mechanical resistance of the welded joints is fundamental. Typically the resistant cross section of the weld bead (S) measured on the interface between the two sheets has to be larger than the thickness of the upper sheet (T_1), while the penetration depth of the weld bead (P) in the lower sheet has to be deeper than half the thickness of the lower sheet (T_2).

3. Other qualitative attributes of the remote laser welded joint. No drop out of the weld bead is allowed on the bottom side of the lower sheet for esthetical reasons, since the bottom side is the sheet face that is coated and painted. Moreover no defects such as pores, inclusions, and voids are allowed as well as surface irregularities have to be limited.

According to the described constraints the problem of realizing good remote laser welded joint when the two zinc coated sheet are spaced by laser dimples is dominated by the following constrains:

$$0.8G \leq H \leq 1.2G \quad (1)$$

$$S \geq T_1 \quad (2)$$

$$\frac{1}{2}T_2 \leq P \leq T_2 \quad (3)$$

In this work due to the relatively novelty of the laser dimpling process the objective function is the maximization of the productivity that means in this simplified context the maximization of the scanning speed in both phases: laser dimpling and remote welding when a single overlapped joints has to be obtained. Aim of the experimentation is to demonstrate the flexibility of the laser dimpling and remote welding processes by pursuing the maximum welding speed while the overall quality of the joint and the required process specification of the chosen case study are preserved. The maximum speed is graphically determined taking into account the area that constrains in Eq. (1-3) delimitate on the space of the process parameters and the natural variability of both phases. The process variability indeed is included by considering in the regression models not the regression function for the mean but the confidence interval for the mean.

Insert Figure 2 here

3. MATERIAL SELECTION AND EXPERIMENTATION DESIGN

The selected case study is based on the technical specifications commonly found in remote laser welding of overlapped zinc coated steels and formulated in Eq. (1-3) when two typical high strength steels are used as upper and lower sheets.
The material of the upper plate is HCT780X+ZE (EN 10346:2009) with a thickness T_1 of 0.75 mm, while the lower plate is DC04+ZE (EN 10152:2009) with a thickness T_2 of 1.5 mm (see Table 1).

An IPG Photonics YLR 1000 active fiber laser source was used for both dimpling and remote laser processes. The laser source has a modular architecture, based on two laser power modules, each one by 500 W of power that results in a maximum output of 1000 W in continuous wave regime.

As for the galvanometric scanner system, an El.En. ThetaFiber prototype was mounted on an ABB IRB2400 robot and was used for both dimpling and welding experimentations. Table 2 summarizes the technical characteristics of the active laser source and the scanning welding system.

The employed laser source generates a multi-mode beam with an M^2 of 5.14 at a central wavelength of 1070 nm. The resulting beam intensity distribution is close to TEM_{00}. The laser beam is convoyed towards the laser scanning system with a delivery fiber with a diameter of 50 μm. The laser beam is then sent into a collimating unit with a focal length of 60 mm, deflected with a couple of Beryllium scanning galvo mirrors and finally focused on the working surface thanks to a theta lens with a focal length of 400 mm. In this configuration the calculated laser beam diameter at focal plane was 333 μm. A view of the equipment used for the remote laser process experiments is presented in Fig. 3.

Insert Table 1 here

Insert Table 2 here

Insert Figure 3 here

3.1. DIMPLING

The physical phenomena behind the laser dimpling process can be explained by the keyhole dynamics generated by a laser pulse with sufficient intensity. If the laser pulse is stationary, the keyhole is closed up at the end of the laser pulse. In this case, the molten metal flows inward from all around the keyhole to form a symmetrical spot weld. Usually no hump can be created in such a way. However by careful observation of a bead on plate weld, it can be noticed that a dip always

exists at the end of the weld. This means that a small amount of material is moved to the adjacent track [22]. Therefore, when the laser pulse is moving, the molten metal flows around the keyhole from keyhole front to its rear. At the end of the laser pulse, a small amount of molten metal solidifies to form a hump due to its momentum. The height of the hump depends on the laser power density, the laser scanning speed (v), the beam profile and the length of the laser trajectory (L) used during the execution of the dimple.

Preliminary tests, here not presented for sake of briefness, were conducted for the identification of a feasibility region for the dimpling process. As summarized in Table 3, a laser beam defocusing of 30 mm was used, leading to a laser beam spot diameter of 711 μm. Also the laser power and the trajectory length were kept at fixed values, respectively 1000 W and 1.55 mm, while the only process parameter used at variable level was the scanning speed of the laser beam over the sample surface that was varied at 4 different levels from 0.5 m/min to 2.0 m/min.

According to the process specifications presented in paragraph 2 and to the thickness of the upper plate T_1 of 0.75 mm, a value for the dimple height H of 100 ± 20 μm was considered as process target for the selected dimpling case; as for the experimental phase, the lower plate DC04+ZE was used.

For each scanning speed 5 replications were executed and the height H was measured for each dimple. The measurements were performed with a focus variation 3D microscope (Alicona Infinite Focus) that also allows representative 3D macro-views of the dimple shapes to be taken.

Insert Table 3 here

3.2. REMOTE WELDING

In the RLW experiments, all the laser process tests were executed on sample plates (25 x 40 mm^2). A single stitch 30 mm long was reproduced at the center of the sample. Samples were clamped according to the scheme presented in Fig. 2, while the correct gap value is warranted by the presence of calibrated spacers with a height of 100 μm inserted laterally to the weld bead position between the overlapped sheets.

As already done for the laser dimpling process, the remote laser welding process experiments were conducted by varying only the laser welding speed. To ensure the maximum performances in terms of laser coupling inside the sample surfaces, the maximum laser power of 1000 W was used on a laser spot focused on the upper surface of the HCT780X+ZE, leading to a spot diameter of 333 μm. The gap between the sheets was controlled by placing calibrated spacers laterally to the weld bead, ensuring a constant gap value of 100 μm. The welding speed was tested at 4 different levels ranging from 1.5 m/min to 6 m/min. A summary of the used process parameters is presented in Table 4.

According to the process specifications presented in section 2 and to the thickness of the upper plate T_1 of 0.75 mm and of the lower plate T_2 = 1.5 mm, the target range for the weld bead penetration was set to 750 μm ≤ P ≤ 1500 μm, while the target range for the resistant cross section S of the weld bead was set to S ≥ 750 μm, For each welding speed 3 replications were performed.

Specimens for microstructural examinations and bead dimension determinations were cut using a precision diamond saw and polished by conventional metallographic techniques, where Nital 2% was used as chemical reagent. The bead dimensions, P and S, were measured on the cross section of the welded joints making use of standard image analysis software. Optical observations were carried out on the prepared specimens to evaluate the other bead qualitative attributes.

Insert Table 4 here

3.3. CONFIRMATION RUNS WITH BOTH LASER DIMPLING AND REMOTE WELDING

In order to validate the combined use of the processing conditions obtained singularly in the laser dimpling and remote welding experiments, a confirmation experiment was executed with the selected optimal process parameters that fulfill the constraints in Eq. (1-3) and allows working at the maximum scanning speed. According to the process scheme presented in Fig. 4, four dimples were prepared on the lower sheet of the DC04 sheet. Then the upper sheet was clamped together and laser welded with a seam track placed in the area limited by the dimples. The same metallographic and measurement techniques mentioned before were used to evaluate the final welded bead dimensions and quality.

Insert Figure 4 here

4. RESULT ANALYSIS

4.1. REMOTE LASER DIMPLING

Representative macro-views of the dimples together with a 2D dimple profile at different scanning speed are shown in Fig. 5. The obtained dimples have a negative-positive profile: a negative cavity is obtained with the molten material moved around the keyhole, a correspondent positive protrusion is left behind.

Fig. 6 shows the individual plots of the measured dimple height H versus the scanning speed. As it can be observed, an increase in the scanning speed leads to a decrease of the dimple height. This behavior can be related to the decrease of the laser-material interaction time and to the consequent lower laser energy that is coupled in the molten material. This results in a lower momentum of the molten material around the keyhole and the process mechanism can be fundamentally compared with keyhole welding; whereby a highly focused power beam produces a vapor cavity in a substrate which is translated through the workpiece, according to the motion of the beam. Traversing the beam across the workpiece creates a trailing melt pool. The combination of surface tension variation along the weld pool and vapor pressure from the cavity causes a displacement of material opposite to the beam's direction of travel. This is evident in keyhole laser welds by the presence of a crater at the end of the weld, and a corresponding bump at the weld initiation point. In particular, the equilibrium state between the keyhole wall and the surrounding molten material is supposed to be dependent on the interaction between the vapor jet from the keyhole formation and the melt, which are a strong function of the melt flow velocity and the keyhole temperature.

Furthermore the explored scanning speed range ensures the dimple height between few μm up to 250 μm, as similarly reported in [22]. On the other hand, wide process variability is observed probably due to the effect of uncontrolled process variables. Such high variability needs further investigation but the uncontrolled thickness of the zinc coating and the roughness of the surface as well as chaotic explosions of the vaporized zinc layer can affect the dimple height.

An appropriate regression model that describes how the dimple height H decreases with the scanning speed is represented by the following equation:

$$H\ [\mu m]\ =\ 105.939/\ v\ [m/min] \quad (4)$$

The performed regression analysis shows a good fitting of the data (R^2_{adj} is over 97%) and no evidence of lack of fit. Standard checks on the normality and homogeneity of variance of the residuals are satisfied as well. The linear regression model of Eq 4 together with 95% of confidence interval about the regression line for the mean expected response of variable H, as well as the lower and upper specification limits are presented in Fig. 7. By considering the 95% confidence interval (CI) for the scanning speed, the range for the scanning speed that ensures the desired dimple height of 100 ± 20 μm is between 1.0 m/min and 1.2 m/min. In fact a scanning speed of 1.0 m/min results in a fitted value of H equal to 105.94 μm while the 95% CI is 95.30 -116.70 μm. On the contrary a scanning speed of 1.2 m/min results in a fitted value of H equal to 88.30 μm while the 95% CI is 80.00 - 97.00 μm. In the last case the lower limit is too close to the lower specification limit. Therefore the lower scanning speed, 1 m/min, was preferred in order to guarantee the dimple height constrain.

Insert Figure 5 here

Insert Figure 6 here

Insert Figure 7 here

4.2. REMOTE LASER WELDING

Representative cross sections belonging to different welding conditions are presented in Fig. 8. No welding defects such as pores and voids are observed in the cross sections of all the weld beads. The upper surface of the samples presents a superficial chamfer whose dimension slightly increases with decreasing welding speed. This defect can be due to the high brightness of the used laser beam that vaporizes a part of the molten material in correspondence of the laser beam axis where the power density is at maximum. This defect can also be attributed to the drop of molten material inside the free space between the overlapped sheets. The increase of the dropped material while the welding speed decreases can be related to the increasing amount of molten metal involved in the fusion process.

A relatively large dimension of the heat-affected zone is observed at the lowest welding speed of 1.5 m/min while lower values are observed at higher welding speed due to the fact that when the speed increases the energy transmitted per unit length decreases. However, no significant welding defects are observed in the heat-affected zone.

As for the geometrical dimensions of the weld bead, such as the weld bead penetration (P) and the resistant cross section (S), their values decrease with the increasing welding speed with minimal values for both P and S at the highest speed of 6.0 m/min (see their individual plots in Fig. 9a and 9b). As expected, an increase of the scanning speed corresponds to a reduction in the energy transmitted to the workpiece and consequently to a reduction in the quantity of the molten material involved in the fusion process.

The measured penetration P was fitted with the following regression model:

$$P\ [\mu m] = 1883.1 - 297.89\ v\ [m/min] \quad (5)$$

where the bead penetration linearly decreases with the scanning speed. The performed regression analysis presents a good fitting of the data (R^2_{adj} is over 94%) and no evidence of lack of fit. Standard checks on the normality and homogeneity of variance of the residuals are satisfied as well.

Since it is fundamental to have sufficient cross section (larger than 750 μm) and contemporaneously avoiding drop out, the range of speeds fulfill the limits is between 1.8 m/min and 3.5 m/min (see the window in Fig. 10).

In fact, by considering a welding speed v = 1.8 m/min, a fitted value for P of 1346.90 μm is expected with a 95% CI between 1207.50 μm and 1487.30 μm. On the other hand, by considering a welding speed of 3.5 m/min, a fitted value for P of 840.50 μm is expected with a 95% CI between 753.00 μm and 928.00 μm. The optimum scanning speed therefore ranges between 1.8 m/min and 3.5 m/min and the final value depends on the analysis of the other dimension, the resistant cross section S.

As for the resistant section S, the linear regression model:

$$S\,[\mu m] = 1099.38 - 108.207\,v\,[m/min] \quad (6)$$

depicts how S decreases while increasing the welding speed, while Fig. 11 shows the correspondent regression line and its 95% confidence interval. The resistant section linearly decreases with the scanning speed and the regression analysis shows a good fitting of the data (R^2_{adj} is over 77%) and no evidence of lack of fit. Standard checks on the normality and homogeneity of variance of the residuals are satisfied as well.

Accordingly to the 95% CI in Fig. 11 a welding speed lower than 2.4 m/min allows the constraint of the minimum resistant section to be fulfilled. Indeed a fitted average value of 839.70 μm is expected while the 95% CI ranges between 749.00 μm and 931.00 μm.

When both dimensions P and S are taken into account, the regression analysis indicates that the specification on weld bead penetration ($T_2/2 \leq P \leq T_1$) is fulfilled for a range of the welding speed between 1.8 m/min ≤ v ≤ 3.5 m/min while the regression analysis indicates that the specification on weld bead resistant section ($S \geq T_1$) is fulfilled for values of scanning speed lower than v ≤ 2.4 m/min (see more details in Table 8). Therefore a scanning speed of 2.4 m/min is the optimum value to be used in the RLW because the maximum productivity is guarantee as well as the respect of the given specifications.

Insert Figure 8 here

Insert Figure 9 here

Insert Figure 10 here

Insert Figure 11 here

4.3. CONFIRMATION RUNS WITH LASER DIMPLING AND WELDING

In the end the two separated experimentations, laser dimpling and remote welding, were validated with the execution of several confirmation runs performed according to the optimized process parameters listed in Table 5. Four dimples were laser welded on the lower sheet with a set distance from the welding trajectory as shown in Fig. 4. After laser dimpling, the dimples were measured (see an example in Fig. 12) and the sheets clamped together. The measured dimples height was 105 ± 12 μm, that is within the given constrains (100 ±20 μm).

The remote laser welding was executed and as previously defined the dimension P and S as well as the quality of the welded beads were measured and evaluated on cross section to the welded joints. Fig. 13 shows the confirmation runs obtained for two replications. Both runs are within the constrain area confirming the validity of the proposed solution. Fig. 13 also shows the macro-views of two weld bead cross section where no welding defects such as pores and voids are observed.

Insert Table 5 here

Insert Figure 12 here

Insert Figure 13 here

5. CONCLUSIONS

In the present paper two key enabling processes for the automotive industry, laser dimpling and remote welding, are investigated together with the aim of realizing an assembling procedure that is accomplished with the same laser scanner head and allow overcoming the problem of the zinc venting. Based on an experimental approach the experimentation has led to the following main results:

- Dimples at a controlled height, that respects the automotive specifications, can be obtained with an appropriate use of the scanner head. Laser dimpling has evident advantages: dimple position, shape and dimensions are not rigid but can be modulated managing the laser beam and scanner head process parameters. No progressive wear of the tool is present, and above all, the productivity is very high thanks to the capability of the scanner head to rapidly move the laser beam over the whole process area.
- When the gap imposed by the automotive specifications is respected, remote laser welded joints with the opportune penetration and resistant section can be obtained at high speed preserving the required bead quality.
- Thanks to the optimization of the laser dimpling and of the remote laser welding processes, the overall quality of the joint process can be considered similar to the one of the traditional resistant spot welding process.

ACKNOWLEDGEMENTS

Authors would like to acknowledge Dr. Manuel Lai of IRIS and Giovanni Masotti of El.En. for their technical support to the research activity. Moreover the authors gratefully acknowledge the financial support from the EU program FoF-ICT-2011.7.4 in the frame of the grant “Remote Laser Welding System Navigator for Eco & Resilient Automotive Factories-RLW Navigator”.

REFERENCES

[1] Hoffmann, P., Kugler, P. , Schwab J., 2003, “Laser Brazing with High Power Solid State Lasers – Systems and Applications in Automotive Industry”, Proceedings of the Second International WLT-Conference on Lasers in Manufacturing, pp.1-4.

[2] Lütke, M., Mahrle, A., Himmer, T., Morgenthal, L., Beyer, E., 2008, “Remote-cutting – a smart solution using the advantages of high brightness lasers”, ICALEO 2008 Congress proceedings, (2008), 695-702.

[3] Buehrle, J., Bea, M., Brockmann, R., 2013, “Laser Remote Process Technology on Automotive Manufacture”, Proceedings of the FISITA 2012 World Automotive Congress, Lecture Notes in Electrical Engineering, 199, pp 89-97.

[4] Zaeh, M., Moesl, J., Musiol, J., Oefele, F., 2010, “Material processing with remote technology - revolution or evolution?” Laser Assisted Net Shape Engineering 6, Proceedings of the LANE 2010, Part 1, Physics Procedia, 5(A), pp. 19-33.

[5] Akhter, R., Steen, W., Watkins, K. 1991, “Welding zinc-coated steel with a laser and the properties of the weldment”, Journal of Laser Applications , 3 (2), pp. 9-20.

[6] Yang, S., Carlson, B., & Kovacevic, R., 2011,”Laser welding of high-strength galvanized steels in a gap-free lap joint configuration under different shielding conditions”, Welding Journal, (90), 8s-18s.

[7] Pan, Y., & Richardson, I., 2011, “Keyhole behaviour during laser welding of zinc coated steel”, Journal of Physics D: Applied Physics , 44 (4).

[8] Li, X., Lawson, S., Zhou, Y., & Goodwin, F., 2007, “Novel technique for laser lap welding of zinc coated sheet steels”, Journal of Laser Applications , 19 (4), 259-264.

[9] Chen, H.-C., Pinkerton, A., Li, L., Liu, Z., & Mistry, A., 2011, “Gap-free laser welding of zinc-coated steel on Al alloy for light-weight automotive applications”, Materials and Design (32), 495-504.

[10] Yang, S., Sarrafi, R., & Kovacevic, R., 2009, “Monitoring of hybrid laser-arc welding of galvanized steels in a gap-free lap joint configuration”, ICALEO 2009 Congress proceedings, pp. 71-78.

[11] Milberg, J., & Trautmann, A., 2009, “Defect-free joining of zinc-coated steels by bifocalhybrid laser welding”, Production Engineering Research Development, (3), 9-15.

[12] Forrest, M., & Lu, F., 1996, “Laser knurling seam preparation for laser welding of zinc coated sheet metal, ICALEO '96 Congress proceedings, pp. 1069-1074.

[13] Forrest, M., Lu, F., 2010, Patent No. US 7693696 B2.

[14] Xie, J., 2002, “Dual beam laser welding”, Welding Journal ,10, pp. 223s-230s.

[15] Iqbal, S., Gualini, M., & Rehman, A., 2010, “Dual beam method for laser welding of galvanized steel: Experimental and prospects”, Optics & Laser Technology , 42, pp. 93-98.

[16] Tzeng, Y.-F., 1999, “Pulsed Nd:YAG laser beam welding of zinc-coated steel”, Welding Journal - Welding, 78 (7), 238s-244s.

[17] Yih-fong, T., 2006, “Gap-free lap welding of zinc-coated steel using pulsed CO2 laser”, International Journal of Advanced Manufacturing Technology, (29), 287-295.

[18] Kraetzsch, M., Standfuss, J., Klotzbach, A., Kaspar, J., Brenner, B., Beyer, E., 2011, “Laser Beam Welding with High-Frequency Beam Oscillation: Welding of Dissimilar Materials with Brilliant Fiber Lasers”, Physics Procedia, 12 pp. 142–149.

[19] Beyer, E., Mahrle, A., Lütke, M., Standfuss, J., Brückner, F., 2012, “Innovations in high power fiber laser applications”, Innovations in high power fiber laser applications, Proc. SPIE 8237, Fiber Lasers IX: Technology, Systems, and Applications.

[20] Thiel, C., Hess, A., Weber, R., Graf, T., 2012, “Stabilization of laser welding processes by means of beam oscillation”, Proc. SPIE 8433, Laser Sources and Applications, 84330V.

[21] T. Schwoerer, Robot-guided remote laser scanner welding for highly-productive welding applications, ICALEO 2008 Congress proceedings, (2008), 392-398.

[22] H.Gu, Laser lap welding of zinc coated steel sheet with laser-dimple technology, Journal of Laser Applications , 22 (3) (2010) 87-91.

[23] A.K.Sinha, D.Y.Kim, D.Ceglarek, 2013, Correlation analysis of the variation of weld seam and tensile strength in laser welding of galvanized steel, Optics and Lasers in Engineering 51 (2013) 1143-1152.

[24] S.Gianmarinaro, S.Riekehr, B.Previtali, M.Hibben, N.Kashaev, 2013, "Mechanical Performance of laser welded and resistance spot welded overlap joints from magnesium AZ31B sheets, Proc. of International Conference on Joining Materials, 5-8 May 2013.

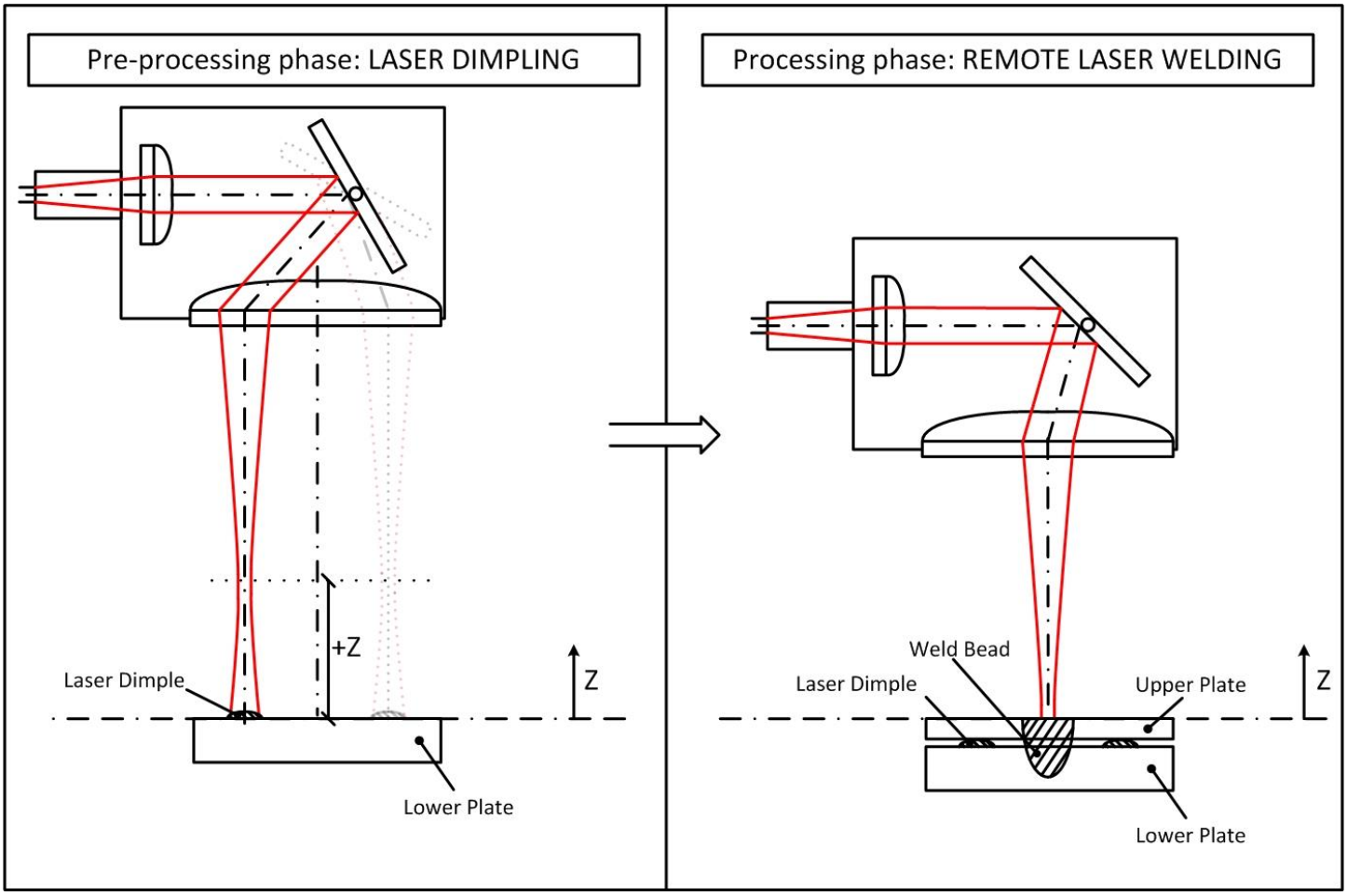

Fig. 1 Sequence of the experimental phases for remote laser welding of zinc coated steels.

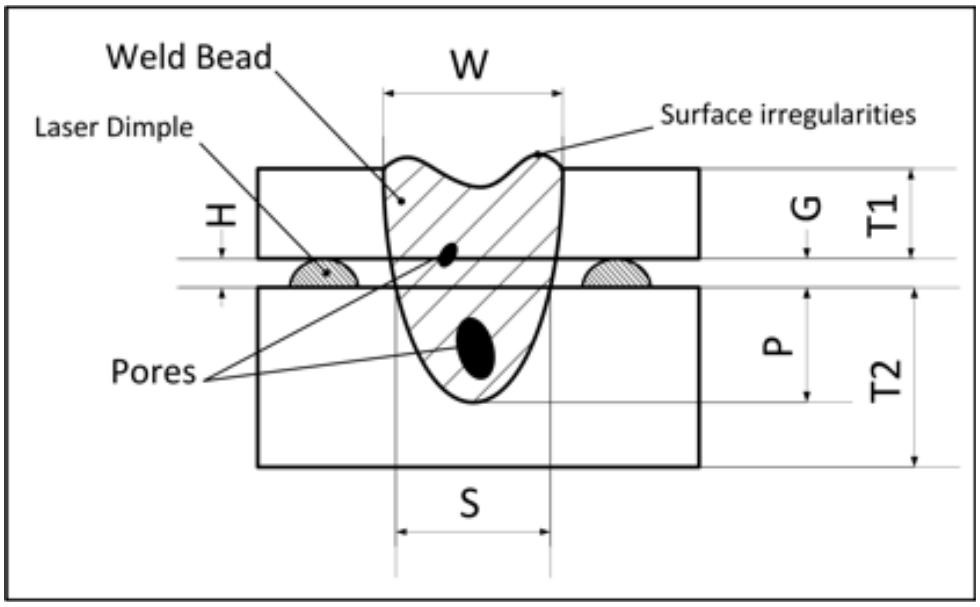

Fig. 2 Configuration of the laser dimpling and remote welding processes.

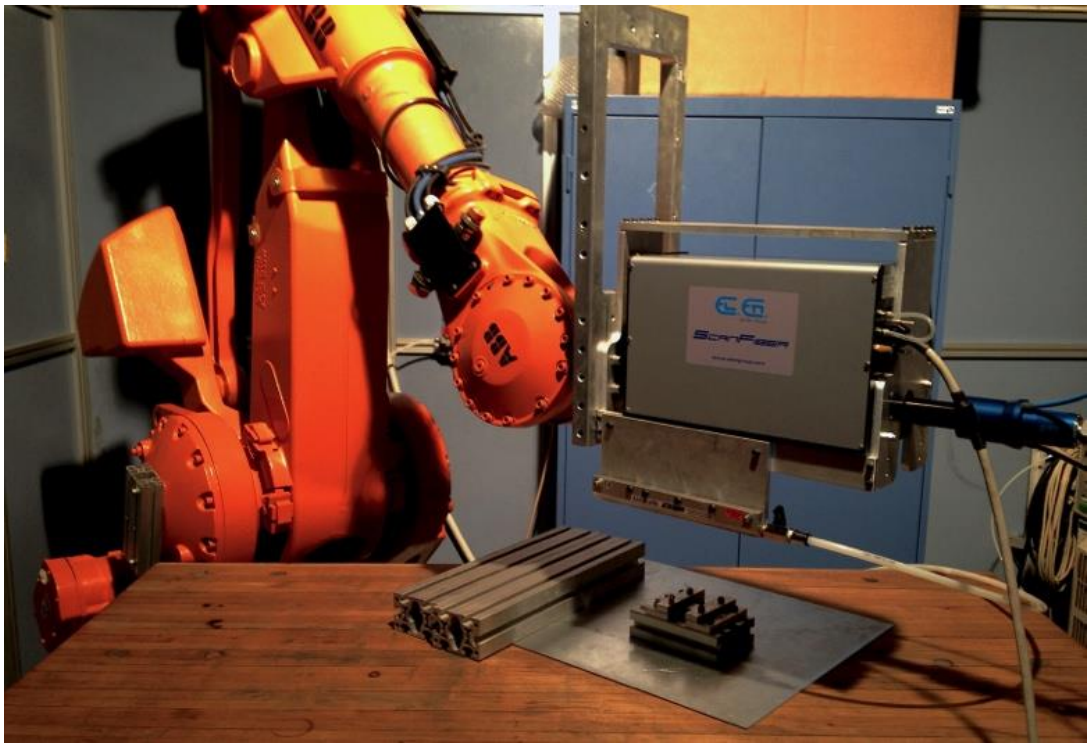

Fig. 3 Overview of the remote laser processing system.

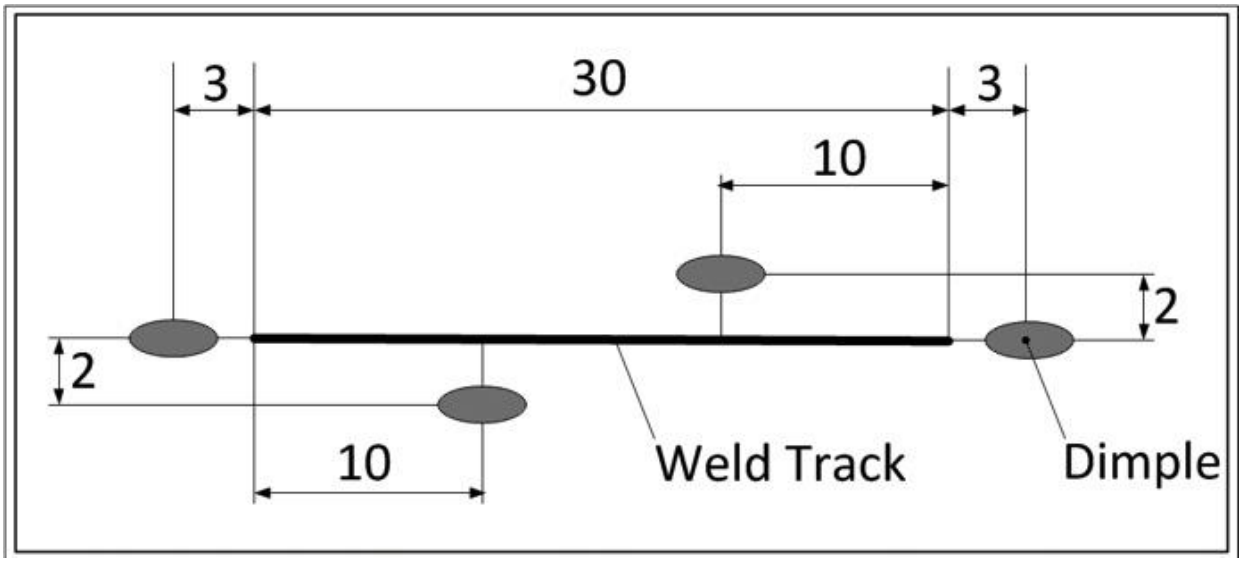

Fig. 4 Configuration of the samples used for the confirmation runs with the relative position of the four dimples close to the welded bead (top view).

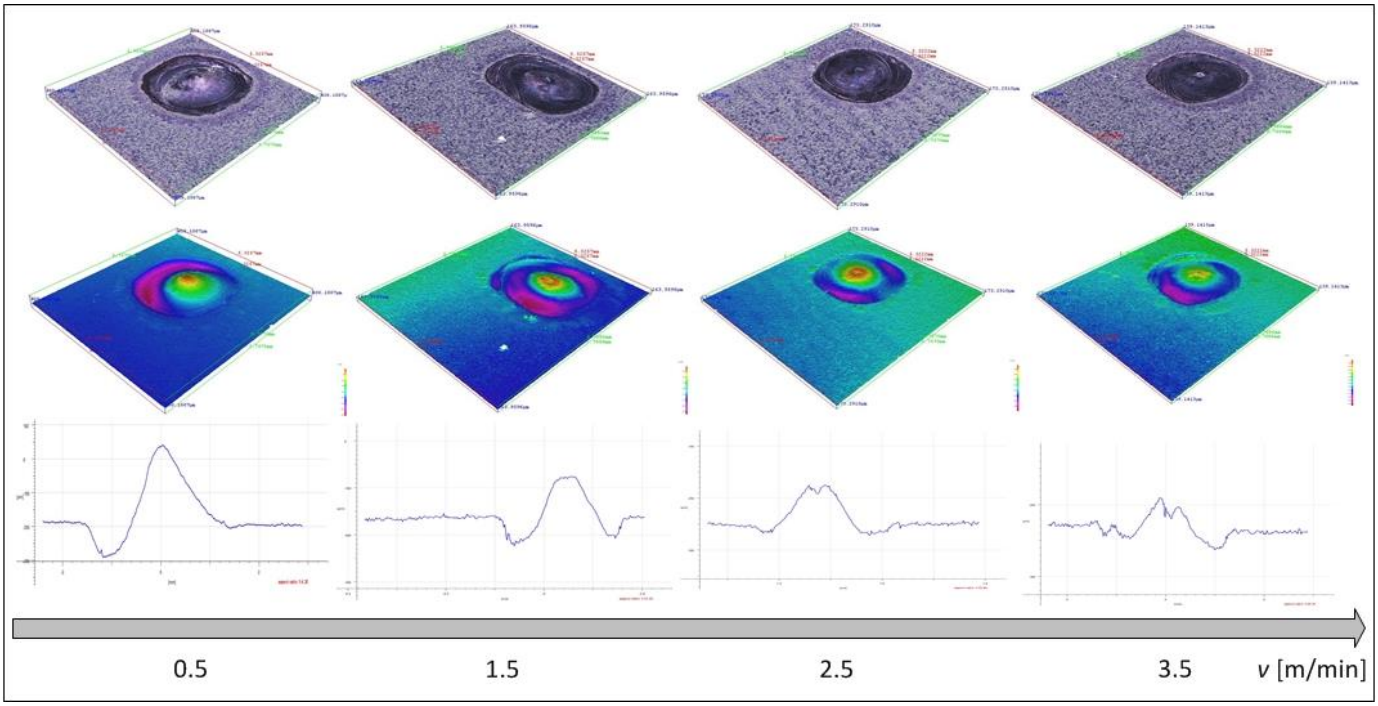

Fig. 5 Dimple shapes at different scanning speeds: macro-view (top); 3D profile (middle) ; 2D cross section profile (bottom)

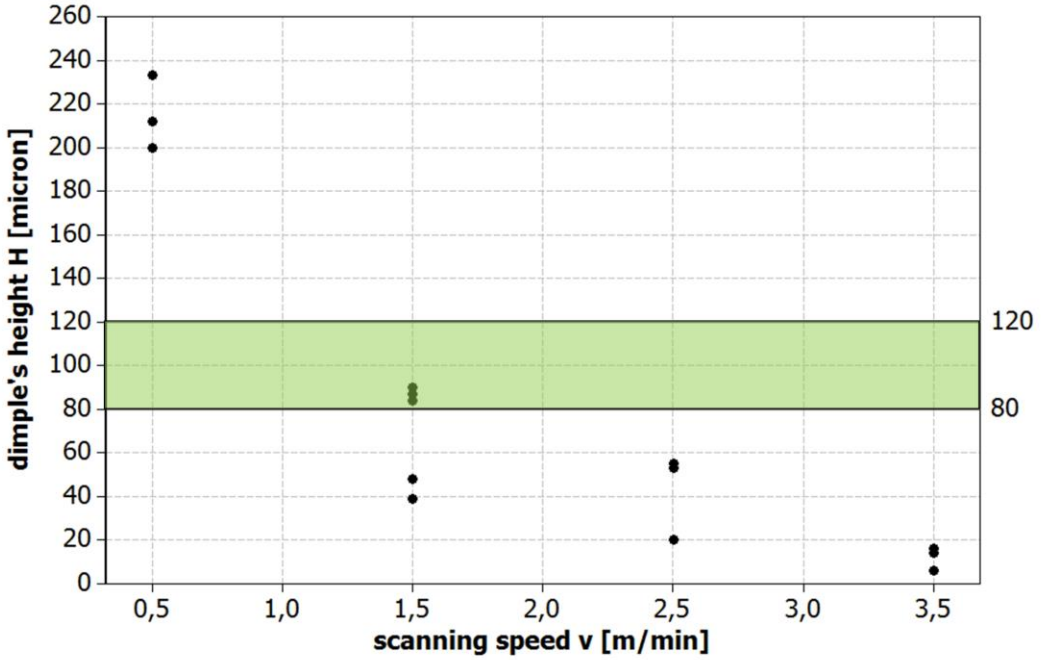

Fig.6 Individual value plot of dimple height versus scanning speed (colored area indicates the admissible range of the dimple height).

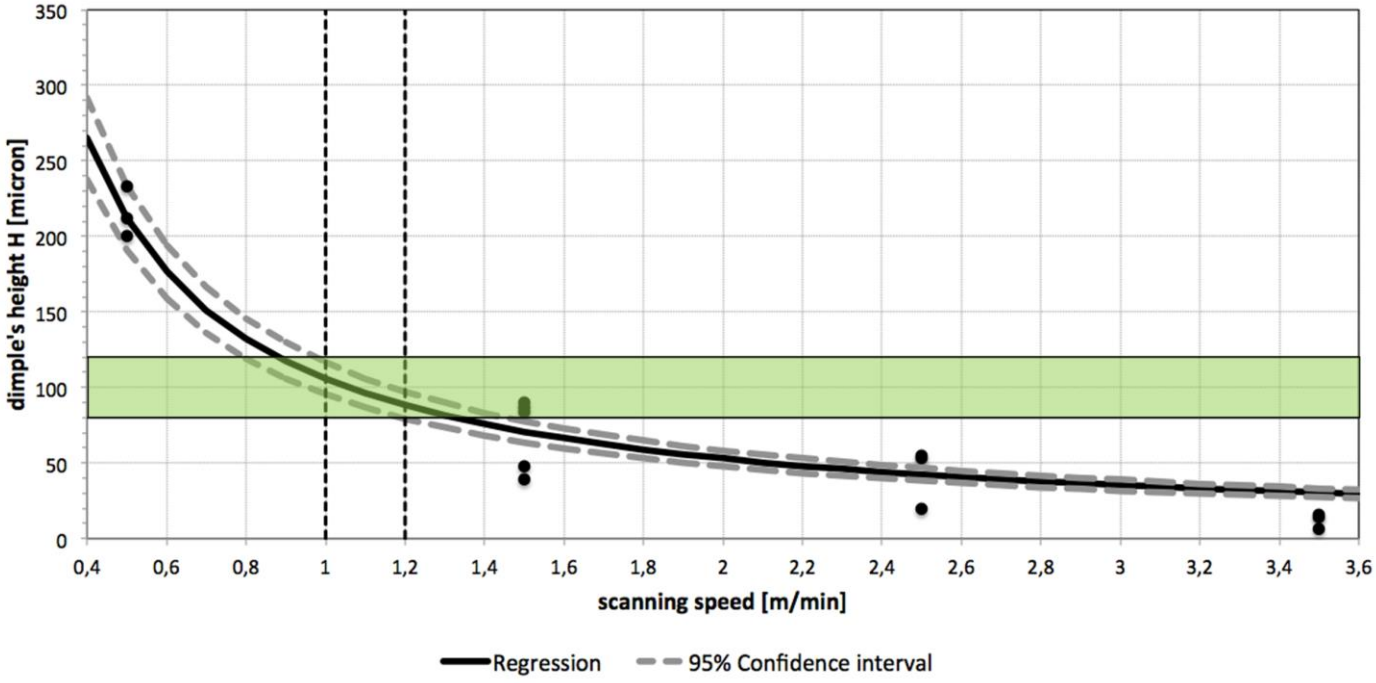

Fig. 7 Regression model of dimple height versus scanning speed (colored area indicates the admissible range of the dimple height).

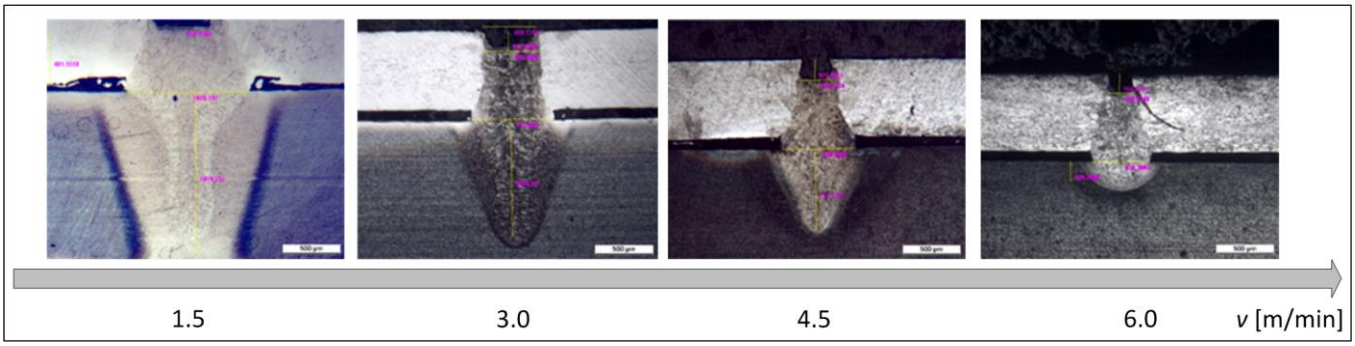

Fig. 8 Representative cross sections of the tested remote laser welding conditions.

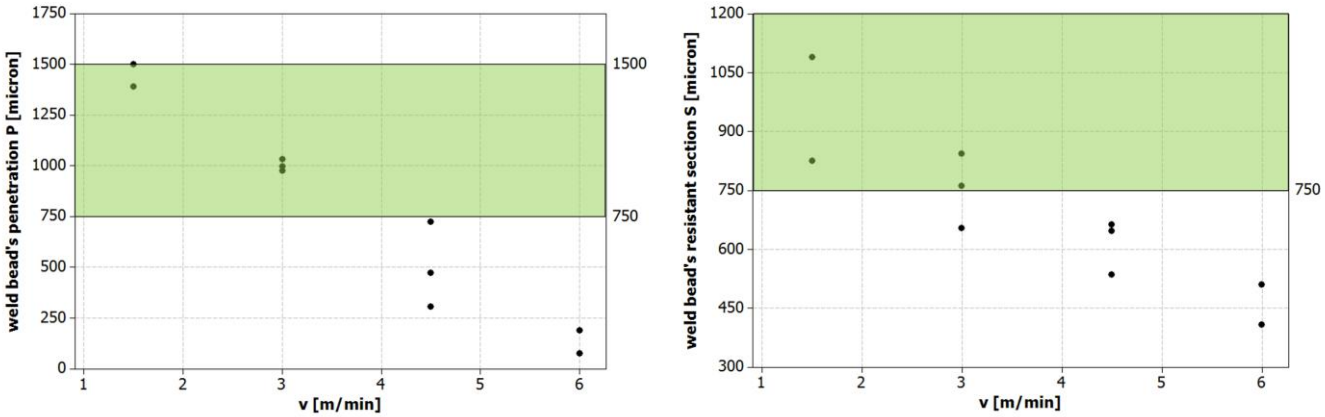

a b

Fig. 9 Individual value plot of weld bead penetration (a) and resistant section (b) versus scanning speed (colored area indicates the admissible range of the penetration and resistant section respectively).

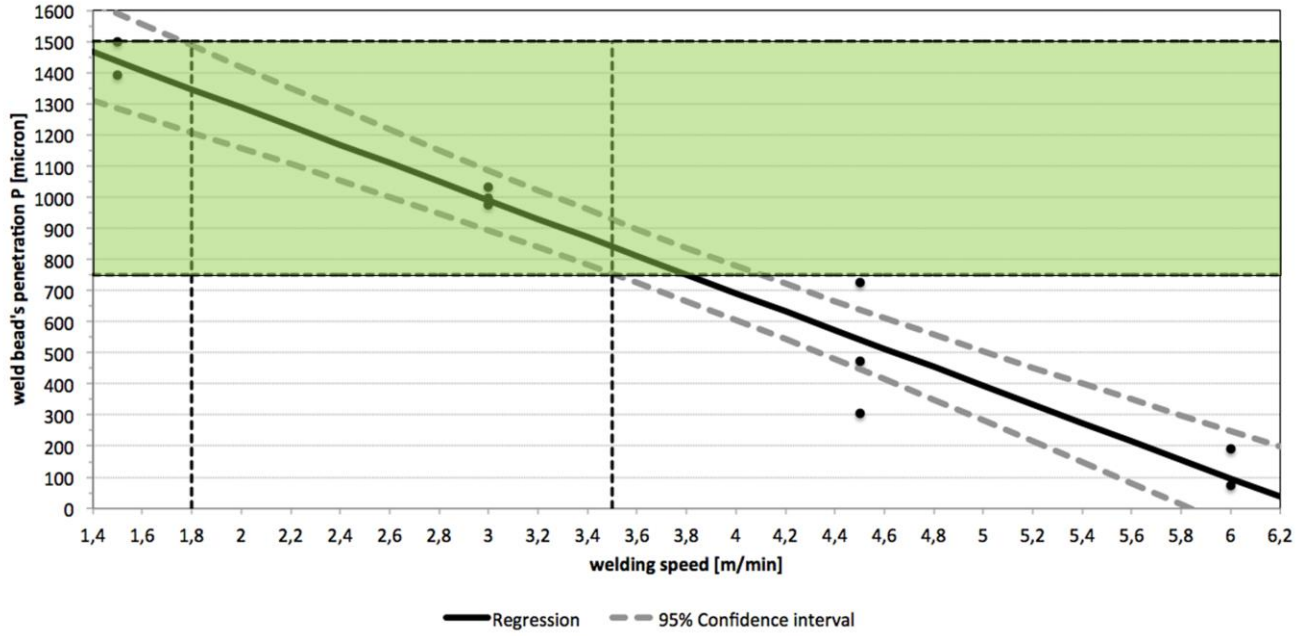

Fig. 10 Regression curve of weld penetration versus scanning speed (colored area indicates the admissible range of the penetration).

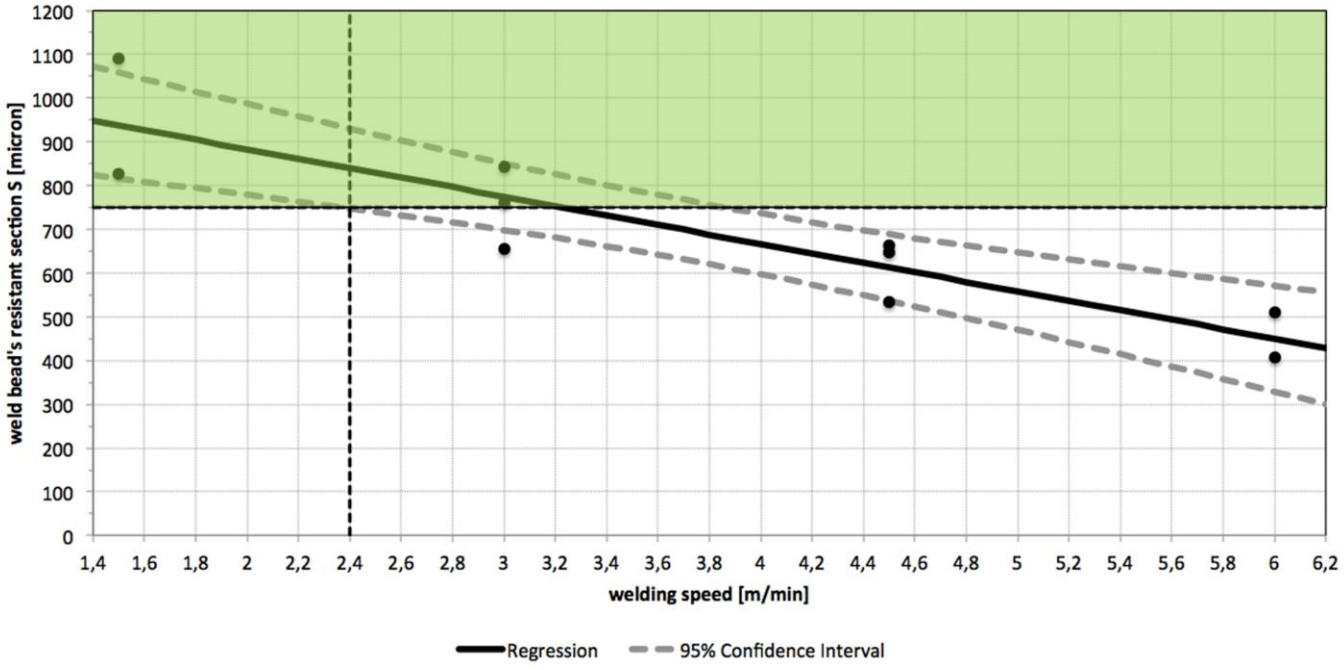

Fig. 11 Regression curve of weld bead resistant section versus scanning speed v (colored area indicates the admissible range of the resistant section).

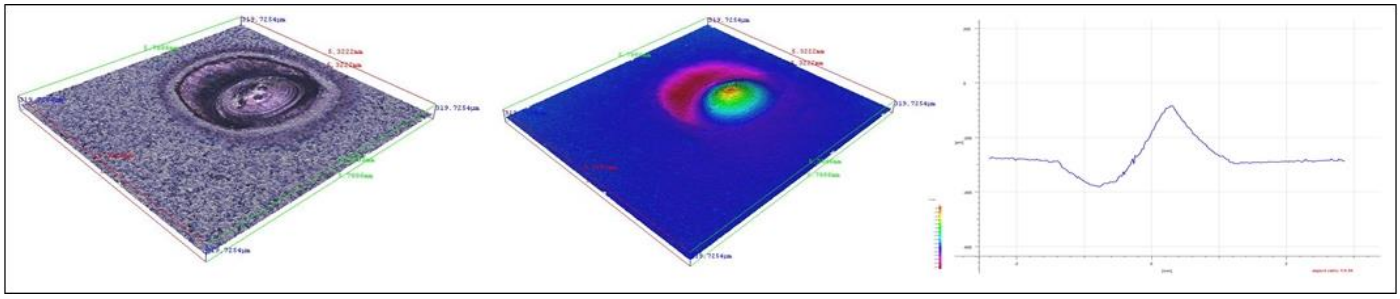

Fig. 12 Confirmation run of the laser dimpling phase: macro-view (lef); 3D profile (middle) ; 2D cross section profile (right)

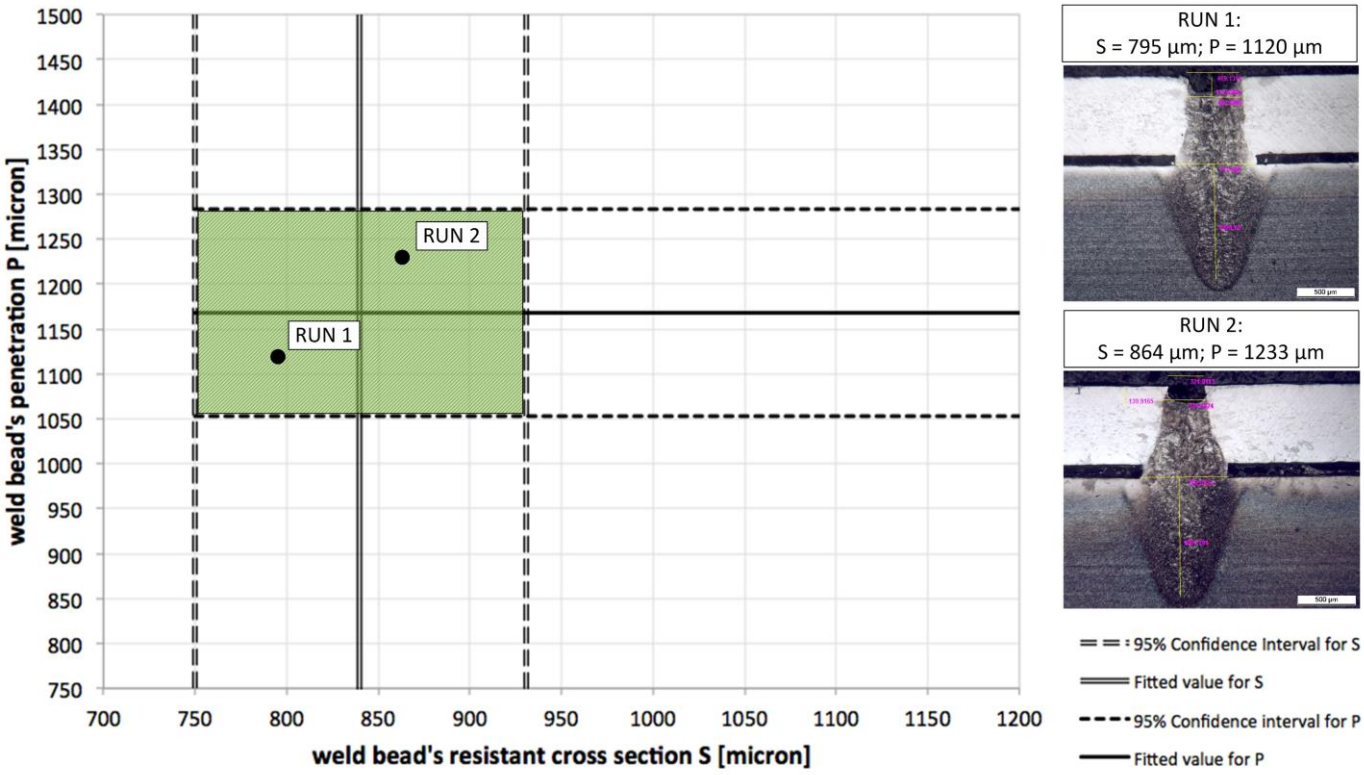

Fig. 13 Confirmation run of the laser welding phase

Table 1 Nominal composition of the materials used in the experiments (wt %).

HCT780X+ZE (EN 10346:2009)							
%C	%Si	%Mn	%P	%S	%Al	%Cr+%Mo	%Fe
0.17	0.80	2.20	0.080	0.015	2.00	1.00	Bal.
DC04+ZE (EN 10152:2009)							
%C	%Mn	%S	%P	%Fe			
0.08	0.40	0.030	0.030	Bal.			

Table 2 Principal technical data of the laser source and scanning welding system.

Fibre Laser Source IPG YLR 1000	
Maximum Laser Power	1000 W, CW
Diameter of Delivery Fiber	50 μm
Laser Wavelength	1070 nm
M^2	5.14
Scanning Welding Head El.En. ThetaFiber	
Scanning Galvo Mirror System	Galvoline G3060, Berilium
Collimating Length	60 mm
Focusing Length - Theta Lens	400 mm
Beam diameter at focal plane	333 μm
Maximum Linear Scanning Frequency	250 Hz
Working Area	200 mm x 200 mm

Table 3 Process parameters used in the experimental phase on dimpling process.

Process Parameter	*Type*	*Value(s)*
Laser Power	fixed	1000 W
Focal Position	fixed	+ 30 mm
Laser trajectory length	fixed	1.55mm
Scanning speed	variable (4 levels)	0.5m/min; 1.0m/min; 1.5m/min; 2.0m/min

Table 4 Process parameters used in the experimental phase on remote laser welding process.

Process Parameter	*Type*	*Value(s)*
Laser Power	fixed	1000 W
Focal Position	fixed	0 mm
Gap between the sheets	fixed	0.1 mm
Welding speed	variable (4 levels)	1.5 m/min; 3 m/min; 4.5 m/min; 6 m/min;

Table 5 Parameters used in laser dimpling and welding processes during the confirmation runs.

Laser dimpling	
Process Parameter	Value
Laser Power	1000 W
Focal Position	+ 30 mm
Laser trajectory length	1.55mm
Scanning speed	1.0 m/min (optimal)
Remote laser welding	
Laser Power	1000 W
Focal Position	0 mm
Weld Track Length	30 mm
Gap between the sheets	0.1 mm
Welding speed	2.4 m/min (optimal)